New Phytologist

Research

The genomics and physiology of abiotic stressors associated with global elevational gradients in *Arabidopsis thaliana*

Diana Gamba[1], Claire M. Lorts[1], Asnake Haile[1,2], Seema Sahay[3], Lua Lopez[1,4], Tian Xia[1], Margarita Takou[1], Evelyn Kulesza[1,5], Dinakaran Elango[5,6], Jeffrey Kerby[7], Mistire Yifru[2], Collins E. Bulafu[8], Tigist Wondimu[2], Katarzyna Glowacka[3] and Jesse R. Lasky[1]

[1]Department of Biology, Pennsylvania State University, University Park, PA 16802, USA; [2]Department of Plant Biology and Biodiversity Management, Addis Ababa University, Addis Ababa, 1176, Ethiopia; [3]Department of Biochemistry and Center for Plant Science Innovation, University of Nebraska-Lincoln, Lincoln, NE 68588, USA; [4]Department of Biology, California State University San Bernardino, San Bernardino, CA 92407, USA; [5]Department of Plant Science, Pennsylvania State University, University Park, PA 16802, USA; [6]Department of Agronomy, Iowa State University, Ames, IA 50011, USA; [7]Aarhus Institute of Advanced Studies, Aarhus University, DK-8000, Aarhus C, Denmark; [8]Department of Plant Sciences, Microbiology and Biotechnology, Makarere University, Kampala, 7062, Uganda

Author for correspondence:
Diana Gamba
Email: dxg5484@psu.edu

Received: *7 June 2024*
Accepted: *29 August 2024*

New Phytologist (2024)
doi: 10.1111/nph.20138

Key words: alpine stressors, *Arabidopsis thaliana*, elevational gradients, genome-wide association studies, genomics, life-history strategies, physiology, regional heterogeneity.

Summary

- Phenotypic and genomic diversity in *Arabidopsis thaliana* may be associated with adaptation along its wide elevational range, but it is unclear whether elevational clines are consistent among different mountain ranges.
- We took a multi-regional view of selection associated with elevation. In a diverse panel of ecotypes, we measured plant traits under alpine stressors (low CO_2 partial pressure, high light, and night freezing) and conducted genome-wide association studies.
- We found evidence of contrasting locally adaptive regional clines. Western Mediterranean ecotypes showed low water use efficiency (WUE)/early flowering at low elevations to high WUE/late flowering at high elevations. Central Asian ecotypes showed the opposite pattern. We mapped different candidate genes for each region, and some quantitative trait loci (QTL) showed elevational and climatic clines likely maintained by selection. Consistent with regional heterogeneity, trait and QTL clines were evident at regional scales (*c.* 2000 km) but disappeared globally. Antioxidants and pigmentation rarely showed elevational clines. High elevation east African ecotypes might have higher antioxidant activity under night freezing.
- Physiological and genomic elevational clines in different regions can be unique, underlining the complexity of local adaptation in widely distributed species, while hindering global trait–environment or genome–environment associations. To tackle the mechanisms of range-wide local adaptation, regional approaches are thus warranted.

Introduction

Changes in environmental conditions with changing elevation are some of the most iconic natural gradients (Caldas, 1966). Correspondingly, changes in plant growth forms are dramatic over hundreds of meters of elevation (Hedberg & Hedberg, 1979; Körner, 2021). Elevational gradients are key drivers of local adaptation, and hence diversity, within species that have broad elevational ranges (Clausen *et al.*, 1940). At high elevations in particular, the combination of cold and high light during vegetative periods poses a major challenge, along with wider fluctuations in daily temperature, decreased partial CO_2 pressure (pCO_2), altered (i.e. orographic) precipitation and clear sky radiation, and shorter growing seasons (Körner, 2003, 2007). While local adaptation to high elevation conditions is documented from reciprocal transplants and common gardens (de Villemereuil *et al.*, 2018; Wos *et al.*, 2022), its physiology and genetic basis is less clear.

High elevation conditions present multiple challenges for photosynthesis. For example, pCO_2 declines approximately linearly with elevation, at 4000 m being only *c.* 65% of sea level pCO_2 (Körner, 2021). Species from high elevations may exhibit higher fitness and better physiological regulation under low atmospheric pCO_2 (Ward & Strain, 1997; Zhu *et al.*, 2010). However, pCO_2 limitation seems counteracted by elevational reductions in pO_2 and photorespiration (Wang *et al.*, 2017), while changes in gene expression in the oxygen-sensing pathway result in suppression of protochlorophyllide at high elevation (Abbas *et al.*, 2022). Additionally, clear sky radiation increases with elevation, but cold temperatures slow the dark reactions of photosynthesis, leading to photo-oxidative damage if excess energy from photons is not properly handled (Wise, 1995). One mechanism to counteract photo-oxidative damage is the increased production of antioxidants (e.g. carotenoids and flavonoids), which scavenge reactive oxygen species (Wise, 1995).

Alpine environments can also experience extreme temperature fluctuations, often reaching below freezing temperature every night, which not only exacerbates oxidative damage but can also physically damage cells (Suzuki & Mittler, 2006).

The model plant *Arabidopsis thaliana* L. (hereafter Arabidopsis) has a broad geographical, environmental, and elevational range, from below sea level to *c.* 4400 m, thus an ideal system for studying multi-regional elevational adaptation. Several studies have addressed elevational adaptation in Eurasia, though in single regions. For example, in Iberia low elevation/coastal sites experience early summer drought, potentially selecting for a drought-escape strategy (Montesinos-Navarro *et al.*, 2011, 2012; Wolfe & Tonsor, 2014; Vidigal *et al.*, 2016). In the Alps, genetic variation in flowering time may contribute to adaptation to seasonal freezing along elevation (Suter *et al.*, 2014), but elevational clines in cold acclimation are unclear (Luo *et al.*, 2015; Günther *et al.*, 2016; Lampei *et al.*, 2019). In the western Himalayas flowering time can be plastic in response to temperature, especially in ecotypes from high elevation (Singh & Roy, 2017). Little is known about elevational clines in African Arabidopsis, where populations are older than most Eurasian, have higher genetic diversity, and grow under the highest recorded elevations (*c.* 2000–4400 m) in the unique Afroalpine ecosystem (Brennan *et al.*, 2014; Durvasula *et al.*, 2017; Brochmann *et al.*, 2021).

One challenge in deriving general conclusions about adaptive responses to elevation for widespread species is that elevational changes in environment often differ from region to region, potentially leading to region-specific local adaptations. For example, while temperature decreases with elevation, different regions may show different elevational gradients in cloudiness/fluctuating light intensity, complicating general patterns at a global scale (Körner, 2021). Even when gradients are consistent, local adaptation to isolated mountain ranges can occur via shared or distinct genetic and phenotypic mechanisms (Bohutínská *et al.*, 2021). For instance, phylogenetic divergence of geographically isolated populations is likely to reduce gene reuse in response to similar selective gradients (Bohutínská & Peichel, 2023; Poore *et al.*, 2023). Furthermore, plant adaptation to extreme conditions often comprises multivariate responses where homeostatic regulation during photosynthesis is achieved in combination with changes in phenology (Kooyers *et al.*, 2015; Fernández-Marín *et al.*, 2020).

We investigated the regional heterogeneity of selection associated with elevation in a widespread model species, integrating Arabidopsis genomes, life history, and physiology. We also sequenced genomes of previously unstudied populations from eastern Africa. Using large-scale experiments and genome-wide association studies (GWAS), we asked:

(**1**) Do high elevation ecotypes show trait differences under high elevation stressors (e.g. faster growth, more efficient resource use, and lower oxidative stress)? Is flowering time variation associated with variation in physiology under high elevation stressors?

(**2**) Is the genome-wide pattern of variation among ecotypes explained by elevational distance, or is geographic distance a better predictor?

(**3**) Are trait–elevation associations consistent among geographic regions? Is there evidence of selection maintaining trait–elevation associations, that is are associations stronger than expected by the genome-wide patterns of variation?

(**4**) Are genes that underlie trait variation under high elevation stress different among geographic regions? Does the allele frequency of quantitative trait loci (QTL) change along elevational gradients?

(**5**) Are the spatial scales of elevational clines associated with the geography of mountainous regions? Are the climatic drivers of QTL-elevation associations different among regions?

Materials and Methods

Natural genotypes and regional variation

To investigate phenotypic and genomic variation across elevational gradients in different regions, we studied 270 ecotypes (i.e. naturally inbred genotypes) of *Arabidopsis thaliana* L. (here Arabidopsis): 232 from the 1001 Genomes Project (ABRC), 21 from Morocco and Tanzania (NASC), and 17 newly collected lines from Ethiopia and Uganda. This panel targeted several elevational gradients, which we classified into five regions according to geographic origin (Supporting Information Dataset S1; Fig. 1a): Asia (n = 77 ecotypes), central Europe (n = 29), northwestern Europe (n = 25), western Mediterranean (n = 112), and the little studied eastern Africa (n = 18). The remaining accessions (nine ecotypes) were from North America and Japan, thus left unassigned, along with a Cape Verde ecotype given its great geographic isolation. Our regional classifications closely followed geography: regions separate different mountain ranges, no mountain ranges were divided, and climatically similar nearby mountain ranges were combined (Notes S1).

To characterize regional elevation–environment gradients, we evaluated environment–elevation associations in each region using linear regressions (R 'lm' function) and examined the environmental axis of variation across regions using principal components analysis (PCA; R 'prcomp' function) and 43 climate variables (Dataset S2). The PCA of bioclimatic variables showed that ecotypes from different regions occupied distinct climates and climatic extremes (Fig. 1b; Notes S1). However, environmental gradients were generally similar, with lower night temperatures and shorter growing seasons at higher elevations (Fig. 1c,d). Based on published flowering time data (Alonso-Blanco *et al.*, 2016), life cycle showed great variation within regions, which was apparent at the level of some major flowering time genes (Fig. S1), suggesting diverse life histories within regions.

Genomic data and population structure

We used a published variant call format (VCF) file (Durvasula *et al.*, 2017) that we concatenated with 16 newly sequenced ecotypes (eight phenotyped) from eastern Africa (Methods S1). To examine population genetic structure, we estimated pairwise genetic distances for the 261 sequenced ecotypes (Dataset S1), with 2409 820 whole-genome resequencing single-nucleotide polymorphisms (SNPs) filtered for linkage disequilibrium (LD:

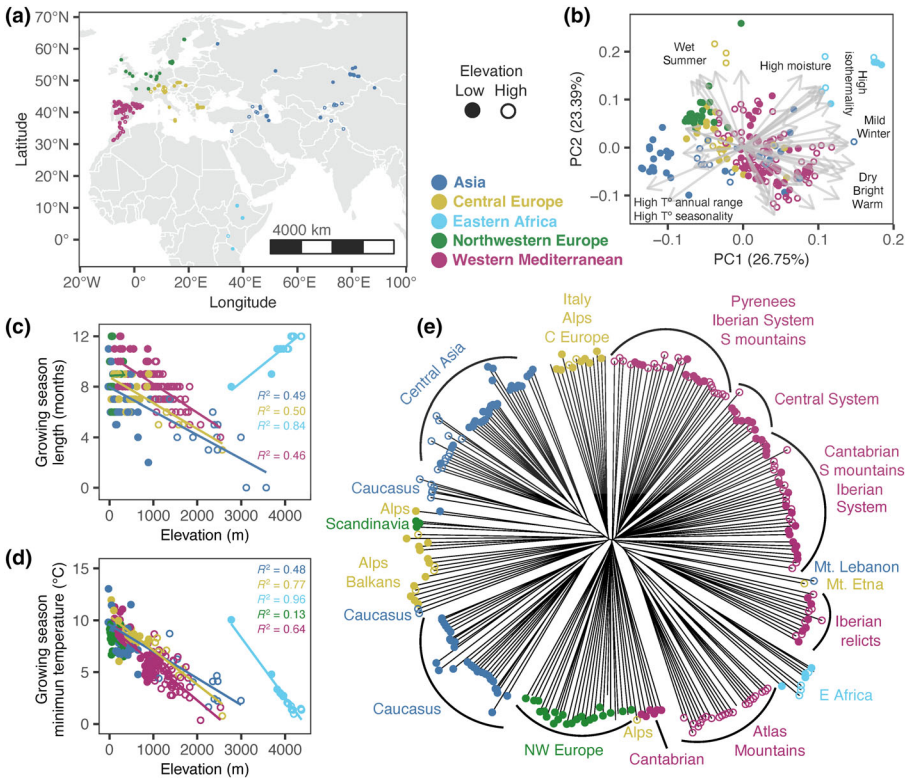

Fig. 1 Provenance, climates, and genetic relationships of studied *Arabidopsis thaliana* ecotypes. Points are ecotypes below (closed circles) and above (open circles) 1000 m above sea level, except for eastern Africa where the threshold is 4000 m. Ecotypes are colored by region with the legend shown between plots (a) and (b). (a) Map with geographic location of ecotypes. (b) Principal components (PC) 1 and 2 of climate space representing conditions in 248 native ecotypes based on 43 climatic variables. Arrows are loadings, with text summarizing loadings more strongly correlated with PC1 and PC2. (c, d) Linear regressions of climate variables on elevation of origin. Selected variables describe the growing season. Significant relationships ($P < 0.01$) are depicted by their coefficient of determination (R^2). (e) Neighbor-joining tree based on 261 ecotypes and 2409 820 resequencing single-nucleotide polymorphisms filtered for linkage disequilibrium (Pearson $r < 0.5$ in 10 kb sliding windows), with annotations of geographic origin. Iberian relicts occur in various Iberian mountains, including the Iberian System, the Central System, and the southern (S) mountains.

Pearson $r < 0.5$ in 10 kb sliding windows). We used the 'snpgdsDiss' function in the SNPRELATE R package (Zheng *et al.*, 2012) to produce a genetic distance matrix, and the 'plotnj' function from APE (Paradis *et al.*, 2004) to plot a neighbor-joining tree.

Population structure largely followed geography in that ecotypes from low and high elevations in the same region were more closely related to each other than to ecotypes of similar elevations on different regions. However, high elevation Caucasus ecotypes were closer to ecotypes from central Asia or to ecotypes from Italy/Balkans (Fig. 1e).

Growth chamber phenotypes

To characterize genetic variation in physiology, resource use, and growth under alpine stressors, we performed three separate experiments with subsets (111–254) of the 270 studied ecotypes. Subsets differed due to seed and space availability and germination success, with a total of 101 ecotypes used in all experiments (60% ecotypes from > 1000 m). To reduce maternal effects, we bulked ecotypes under controlled conditions (Methods S2). Experiments were performed in a reach-in growth chamber (PGC-40L2; Percival Scientific, Perry, IA, USA) with a 12-h photoperiod. Our experimental conditions mimicked alpine conditions of low pCO_2, high light, and night-time freezing (Körner, 2021).

Our first experiment imposed low pCO_2, cool, and bright conditions on 253 ecotypes (Dataset S3). We grew four to five replicates under 200 ppm CO_2 (the approximate preindustrial pCO_2 at 3000 m) for 156 d, at which point plants were harvested and phenotyped (Methods S3). We measured root diameter, rosette diameter, rosette compactness, and $\delta^{13}C$ and $\delta^{15}N$, two stable isotope ratios associated with carbon/water and nitrogen use, respectively, that are integrated across the plant life span. For 80 ecotypes that varied in elevation of origin, we quantified stomatal density.

Our next two experiments imposed contrasting light levels (250 vs 600 μmol m^{-2} s^{-1}) on 111–114 ecotypes (performed simultaneously under cool conditions) (Dataset S4) and contrasting night temperatures (−4 vs 4°C) on 170–172 ecotypes (performed sequentially under bright conditions) (Dataset S5). We grew six replicates for 82–89 d and 72–75 d, respectively, and then, plants were harvested and phenotyped. We measured fresh aboveground biomass, antioxidant activity, leaf color, plasticity in antioxidant activity and in leaf color (i.e. trait difference between conditions), and survival rate (Methods S4). We quantified color because it may capture variation in pigments, which may inform elevational adaptation as pigments act as antioxidants under high light and/or cold (Havaux & Kloppstech, 2001).

When trait measurements could be obtained from multiple replicates, we computed the best linear unbiased estimates with the 'BLUE' function from the POLYQTLR package. Due to tissue availability, for stable isotopes and antioxidant activity, we pooled tissue from all replicates and obtained a collective value per ecotype. Phenotypes were measured in adult preflowering plants.

Q1. Physiology association with elevation and life history To assess how physiology changes with elevation under alpine stress,

we first examined coordinated variation of growth chamber phenotypes with a PCA, separately for our three experiments. We then evaluated life history–physiology covariation with published flowering time data (Alonso-Blanco *et al.*, 2016) and examined trait–elevation covariation, using the Pearson correlation coefficient (95% confidence level) with the functions 'cor.mtest' and 'corrplot' in the CORRPLOT R package (Wei & Simko, 2021). Published flowering times in plants grown under 10 and 16°C were strongly correlated; here, we focus on flowering time at 16°C, which showed greater variation. Because global associations with elevation might be obscured by phenotypic differentiation between isolated regions, we inspected regional differences in trait variation with ANOVA and a Tukey HSD.

Q2. Genomic turnover along elevation vs geographic distance To assess the degree to which genomic composition (18.3 M genome-wide SNPs in 1014 ecotypes) followed isolation-by-distance vs elevation, we modeled genetic distance using linear mixed models implemented in ResistanceGA (Peterman, 2018), together with linear models (for interpretability of R^2 differences). We modified the 'MLPE.lmm' function to allow multiple regression, with terms for geographic distance and elevational difference between genotypes, where random effects are included to account for nonindependence among multiple pairwise observations from the same genotype (Clarke *et al.*, 2002; Gutaker *et al.*, 2020). We compared models using AIC.

Q3. Regional trait–elevation associations To understand how regional elevational gradients shape phenotypes, we tested for region-specific phenotype-elevational clines with linear mixed models that controlled for genome-wide similarity among ecotypes. We used the 'snpgdsIBS' function in SNPRelate to produce an identity-by-state matrix (from 12.1 M genome-wide SNPs in 261 ecotypes), which was a random effect in our models. When significant, these models suggest that selection associated with a given trait is driving clines, because the cline is stronger than expected by the genome-wide cline. To fit models, we used the function 'lmekin' in the KINSHIP2 R package (Therneau, 2012). To assess the role of sample size differences among regions, we randomly subsampled the western Mediterranean to $n = 30$ 10 times, in comparison with other regions. For mountain ranges of interest, we also examined local phenotype-elevational clines.

Q4. GWAS, functional annotation, and analysis of QTL We identified QTL for alpine stress phenotypes with GWAS that controlled for kinship on our global dataset ($n = 110$–253 ecotypes; Dataset S6a), and on regional datasets for phenotypes that significantly varied with elevation ($n = 76$–110), including flowering time ($n = 110$–183; Dataset S6b). We used univariate linear mixed models in GEMMA v.0.98.3 (Zhou & Stephens, 2012), excluding loci with MAF < 0.05 for each trait (*c.* 2.5–2.8 M SNPs), with a false discovery rate (FDR) of 0.05 on Wald test *P*-values. We assigned top SNPs (those with the lowest 100 *P*-values for each trait) to candidate genes using the Araport11 reannotation (Cheng *et al.*, 2017) and a 10-kb window (Datasets S7–S10). Elevational allele frequency clines in GWAS QTL were examined with similar mixed models used for testing trait–elevational clines.

To further evaluate QTL function, we inspected GWAS SNP correlations with gene expression (RNA-seq dataset from Kawakatsu *et al.*, 2016) and performed enrichment analyses. We tested for over-represented GO terms in the 100 top genes detected for traits of interest, using PlantRegMap GO Term Enrichment (Tian *et al.*, 2019) that relies on The Arabidopsis Information Resource (TAIR) database (Lamesch *et al.*, 2012).

Q5. Spatial scale and climate drivers of elevational clines To further characterize changes in elevational clines, we modeled spatial variation in trait–elevation relationships for traits that had major among-region differences in clines (as described in the previous section). First, we implemented generalized additive models (GAMs) with smooth, spatially varying coefficients for the elevation effect on traits, using the MGCV R package (Wood, 2011). The smooth spatial change in elevational effects depending on ecotype location across the study area avoids potential biases in testing for differences in clines among arbitrarily defined regions (DeLeo *et al.*, 2020; Yim *et al.*, 2023). We examined regions where trait–elevation clines had opposite signs and their 95% CIs excluded zero (considered significant).

To identify the spatial scales over which clines changed, we calculated change in the correlation between elevation and traits including ecotypes at increasing distances from focal regions. For focal regions, we selected locations with particularly strong trait–environment relationships. We selected two sites with distinct clines on opposite sides of the Arabidopsis range in Spain and Russia.

To identify climatic gradients most predictive of QTL-elevational clines, we tested QTL genotype–environment associations, *that is* allele frequency correlations with environment (Lasky *et al.*, 2023) for the 19 Bioclim CHELSA variables (Karger *et al.*, 2020) using gemma. For traits with particularly strong regional phenotypic clines, we also conducted enrichment tests to determine with the top 1000 trait-associated SNPs in those regions also showed higher than the genomic background climate associations (permutation-based null model) (Hancock *et al.*, 2011; Lasky *et al.*, 2014).

Results

We found substantial natural genetic variation in all phenotypes. In our experiments with contrasting light or temperature, traits were significantly different between treatments ($P < 0.05$; Notes S2; Fig. S2). Under cool temperatures and high light, plants were smaller, had higher antioxidant activity, and dark purple (vs green) leaves compared with low light. Survival was slightly but significantly lower under high than low light (93% vs 96%). Under bright conditions and night freezing, plants were larger, had higher antioxidant activity, and more orange (vs yellow) leaf extracts than when grown with night temperatures just above freezing. Survival was significantly lower under night freezing (76% vs 100%).

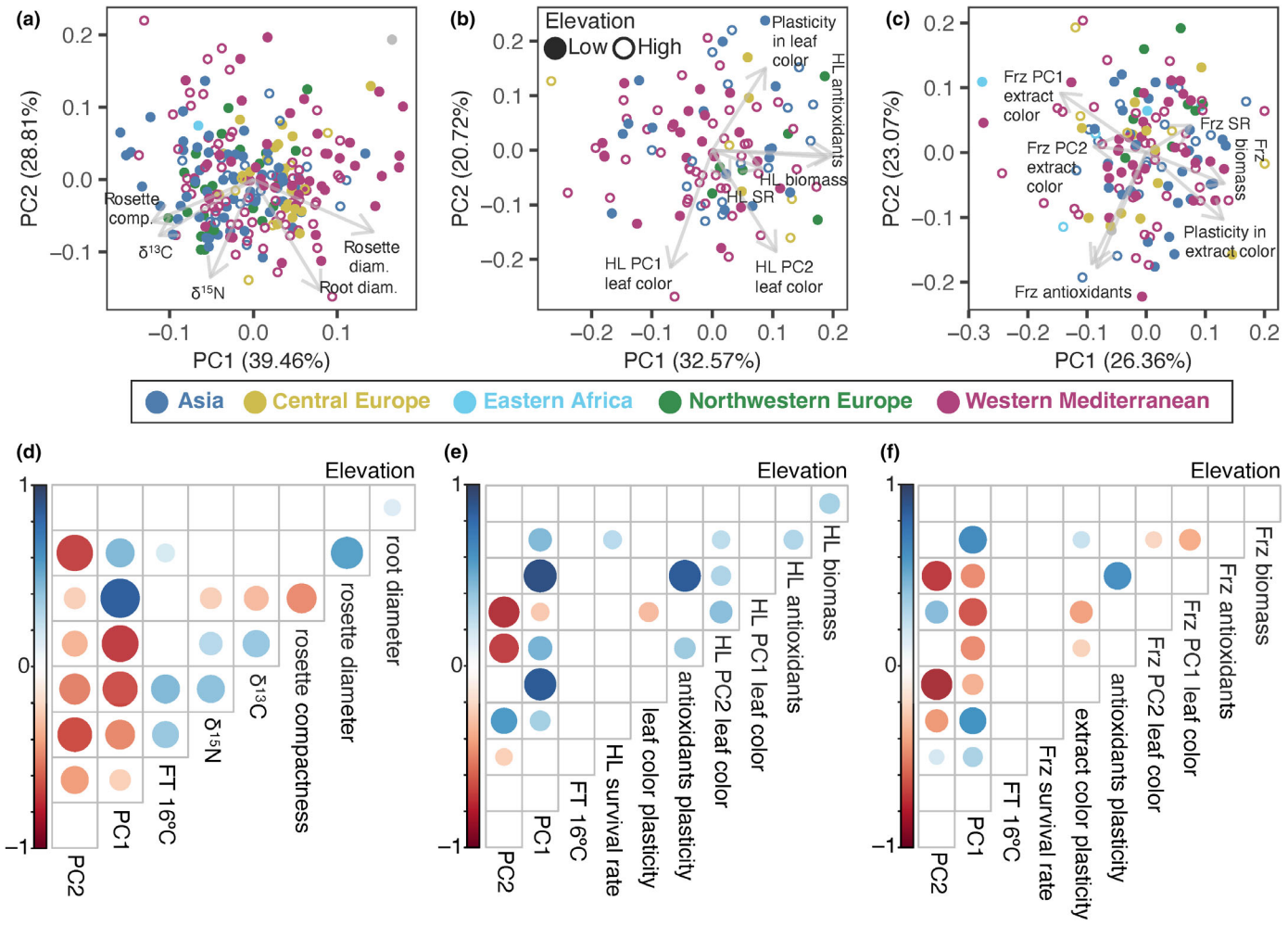

Fig. 2 Natural genetic variation and covariation of *Arabidopsis thaliana* phenotypes in three experiments simulating alpine stress. Eigenvector plots of the loadings of (a) five variables onto principal components (PC) 1 and 2 of phenotypes under low partial CO_2 pressure (pCO_2) conditions in 241 ecotypes (*c*. 38% of which are > 1000 m above sea level; comp. = compactness, diam. = diameter), (b) seven variables onto PC1 and PC2 of phenotypes under high light and cool conditions (HL) in 106 ecotypes (*c*. 58% of which are > 1000 m), and (c) seven variables onto PC1 and PC2 of phenotypes under night freezing and bright conditions (Frz) in 144 ecotypes (*c*. 47% of which are > 1000 m). The two arrows/loadings for antioxidants in (b) and (c) correspond to antioxidant activity and plasticity in antioxidant activity (i.e. difference in antioxidants between high and low light conditions). Points are ecotypes below (closed circles) and above (open circles) 1000 m, except for eastern Africa where the threshold is 4000 m. Ecotypes are colored by region with the legend displayed below eigenvector plots. (d–f) Correlation plots (Pearson *r*) showing significant associations ($P \leq 0.05$) between our experimental phenotypes, corresponding PC1 and PC2, flowering time (FT) under 16°C, and elevation of origin under low pCO_2, high light, and night freezing, respectively. Colors indicate the direction of correlations, and darkness and size of circles represent the strength of associations.

Delayed flowering and resource use efficiency were correlated, but no global strategy in alpine ecotypes

Traits showed covariation under alpine stressors (Fig. 2a–c), resource use traits changed with flowering time, but traits were rarely associated with elevation range-wide (Fig. 2d–f). Under low pCO_2 with cool and bright conditions, ecotypes with compact rosettes had higher $\delta^{13}C$ and $\delta^{15}N$ and were smaller, while larger rosettes were associated with larger roots (Fig. 2a,d). Also, $\delta^{13}C$ and $\delta^{15}N$ were positively correlated with flowering time (Fig. 2d). Under cool temperatures and high light, ecotypes with larger rosettes had higher antioxidant activity, blue content in leaves, and survival (Fig. 2b,e). Under high light and night freezing, larger rosettes had more orange in leaf extracts (Fig. 2c,f).

The only global trait–elevation association we detected was under cool temperatures and high light, where ecotypes from higher elevation had bigger rosettes across regions (Fig. 2e). In many instances, trait means and covariation among traits differed among regions (Notes S3), which together with the distinct regional climates (Fig. 1b), suggests different regional environmentally responsive strategies.

Isolation-by-distance, not elevation, explained genome-wide patterns of variation

Models of genetic distance among ecotypes showed that geographic distance was a stronger predictor than elevational difference, with a few exceptions (linear models: geographic distance

R^2 = 0.08; elevational difference R^2 = 0.01). Mixed models of all ecotypes showed that an isolation-by-distance and elevation difference model (AIC = −1584 537) improved over models including only the distance (AIC = −1584 304) or elevational difference (AIC = −1572 148) and the null model (AIC = −1571 361), indicating that population structure, to a limited extent, follows elevation. Specifically in the Caucasus, the elevational difference only model was favored (AIC = −1612), highlighting the strong elevational turnover in ancestry there (distance-only AIC = −1445, distance and elevational difference AIC = −1610, null AIC = −1410; linear models: geographic distance R^2 = 0.02; elevational difference R^2 = 0.28). However, in the western Mediterranean, AIC of mixed models favored a geographic distance model only (AIC = −79896.04) compared with the other models (elevational difference only AIC = −79323.21, distance and elevational difference AIC = −79894.18, null AIC = −79263.75; linear models: geographic distance R^2 = 0.04; elevational difference R^2 = 0.01). The generally lower AIC values for the distance-only models compared with elevational difference indicate the much greater importance of geographic distance than elevation for population structure: mountain tops in separate regions are genetically distinct.

Trait–elevation clines changed between regions

In general, linear mixed models that accounted for the genome-wide pattern of variation showed that putatively adaptive clines were not consistent among regions and, in some prominent cases of ecologically important traits, were opposite in sign (Fig. 3). Below we report *P*-values from mixed models, and the corresponding linear R^2 of trait–elevation regressions.

In the western Mediterranean flowering time, $\delta^{13}C$, $\delta^{15}N$, and rosette compactness showed positive clines (R^2 = 0.3, 0.3, 0.02, 0.2, respectively, $P < 0.002$; Fig. 3a–d). These clines were generally conserved in different Iberian mountains (R^2 = 0.2–0.7, $P < 0.02$, n = 12–54; Fig. S3a), but not significant in the Iberian System ($P > 0.25$, n = 18–26) and in the Moroccan Atlas ($P > 0.3$, n = 22). Also, the flowering time, $\delta^{13}C$, and rosette compactness clines remained significant using random subsamples of n = 30 western Mediterranean ecotypes (Table S1). The only consistent cline between the western Mediterranean and Asia was greater fresh aboveground biomass for alpine ecotypes under cool high light conditions (R^2 = 0.2 in both regions, $P < 0.04$; Fig. 3g).

In Asia, the flowering time cline was negative (R^2 = 0.1, P = 0.2; Fig. 3a), both in the Caucasus (R^2 = 0.1, P = 0.009, n = 39) and central Asia (R^2 = 0.3, $P = 9.6 \times 10^{-5}$, n = 39), but clines in other traits were different between mountains (Fig. S3b). In Caucasus ecotypes, $\delta^{13}C$ and rosette compactness increased with elevation (R^2 = 0.1 and 0.5, respectively, $P < 0.04$, n = 36), while in central Asia, $\delta^{13}C$, $\delta^{15}N$, and rosette compactness, decreased with elevation (R^2 = 0.2–0.3, $P < 0.001$, n = 36–37). Rosette diameter increased with elevation, but only in central Asia (R^2 = 0.3, $P = 4 \times 10^{-5}$, n = 37).

Flowering time-elevation clines were not significant in central and northwestern Europe, but $\delta^{13}C$ increased with elevation in central Europe (R^2 = 0.1, P = 0.03) and decreased with elevation in northwestern Europe (R^2 = 0.2, P = 0.02; Fig. 3b). In central Europe, this trend was consistent, though not significant, in the Alps (P = 0.07, n = 14) and the Balkans (P = 0.4, n = 8). However, in northwestern Europe, the $\delta^{13}C$-elevation negative cline was driven by the higher elevation non-Scandinavian ecotypes (n = 13) that also had lower $\delta^{13}C$, while in Scandinavian ecotypes we detected a coastal (lower elevation) to inland (higher elevation) positive $\delta^{13}C$-elevation cline (R^2 = 0.3, P = 0.004, n = 12). In general, $\delta^{13}C$ was highest in northwestern Europe (Notes S3), congruent with previous findings of higher water use efficiency (WUE) at higher latitudes (Dittberner *et al.*, 2018).

Antioxidants and pigmentation rarely changed with regional elevation. Afroalpine ecotypes represented the highest part of the Arabidopsis range (mostly 3691–4374 m, with one ecotype at 2775 m). Although based on a limited sample size of seven, unlike other regions, antioxidant activity under night freezing seemed to increase with elevation (R^2 = 0.5, P = 0.005, but Pearson's two-sided P = 0.06). By contrast, in central Europe ecotypes antioxidant activity under night freezing decreased with elevation (R^2 = 0.3, P = 0.01; Fig. 3k).

Putative QTL changed between regions

We report candidate genes with annotated functions that we hypothesized were related to phenotypes (Table 1; Fig. S4), and results from a Gene Ontology enrichment analysis on top GWAS genes (Table S2a–e).

In our global dataset, we mapped two QTL associated with antioxidant activity under high light (FDR = 0.001). The top QTL (composed of 1 SNP) tagged *Ferric Reduction Oxidase 7* (*FRO7*; AT5G49740) and was upstream (in the putative promoter region) of *FRO6* (AT5G49730), both involved in iron chloroplast uptake and expressed in aerial green tissue (Jeong *et al.*, 2008; Jeong & Connolly, 2009; Jain *et al.*, 2014). *FRO6* expression is light-dependent, with several light-responsive elements in the promoter region (Feng *et al.*, 2006). The second top QTL (composed of 2 SNPs) was downstream of a phosphate transporter (*PHT4;4*; AT4G00370) that carries ascorbate into the chloroplast (Miyaji *et al.*, 2015). *PHT4;4* expression is higher in the chloroplast envelope membrane and increases under high light stress, with knockouts having lower levels of reduced ascorbate (an antioxidant) in the leaves, and lower content of ascorbate-dependent xanthophylls and ß-carotene after high light exposure (Miyaji *et al.*, 2015). SNP variants (chr5: 20206030 bp for *FRO6/FRO7* and chr4: 160735 bp for *PHT4;4*) associated with low antioxidant activity were globally uncommon (allele frequency AF = 0.09 and 0.08, respectively), but dominant (AF = 0.81 and 0.84) in high elevation (> 1000 m) Moroccan ecotypes, and infrequent (AF = 0.13 for chr5: 20206030 bp) to rare (AF = 0.03 for chr4: 160735 bp) in Iberian ecotypes (Notes S4). These SNPs did not follow an elevational pattern in models that accounted for kinship (Fig. S5). However, top SNP and gene expression were significantly correlated (unlike in other QTL), but only in the western Mediterranean (Pearson r = 0.2, P = 0.02 for chr4: 160735 bp and *PHT4;4* and Pearson

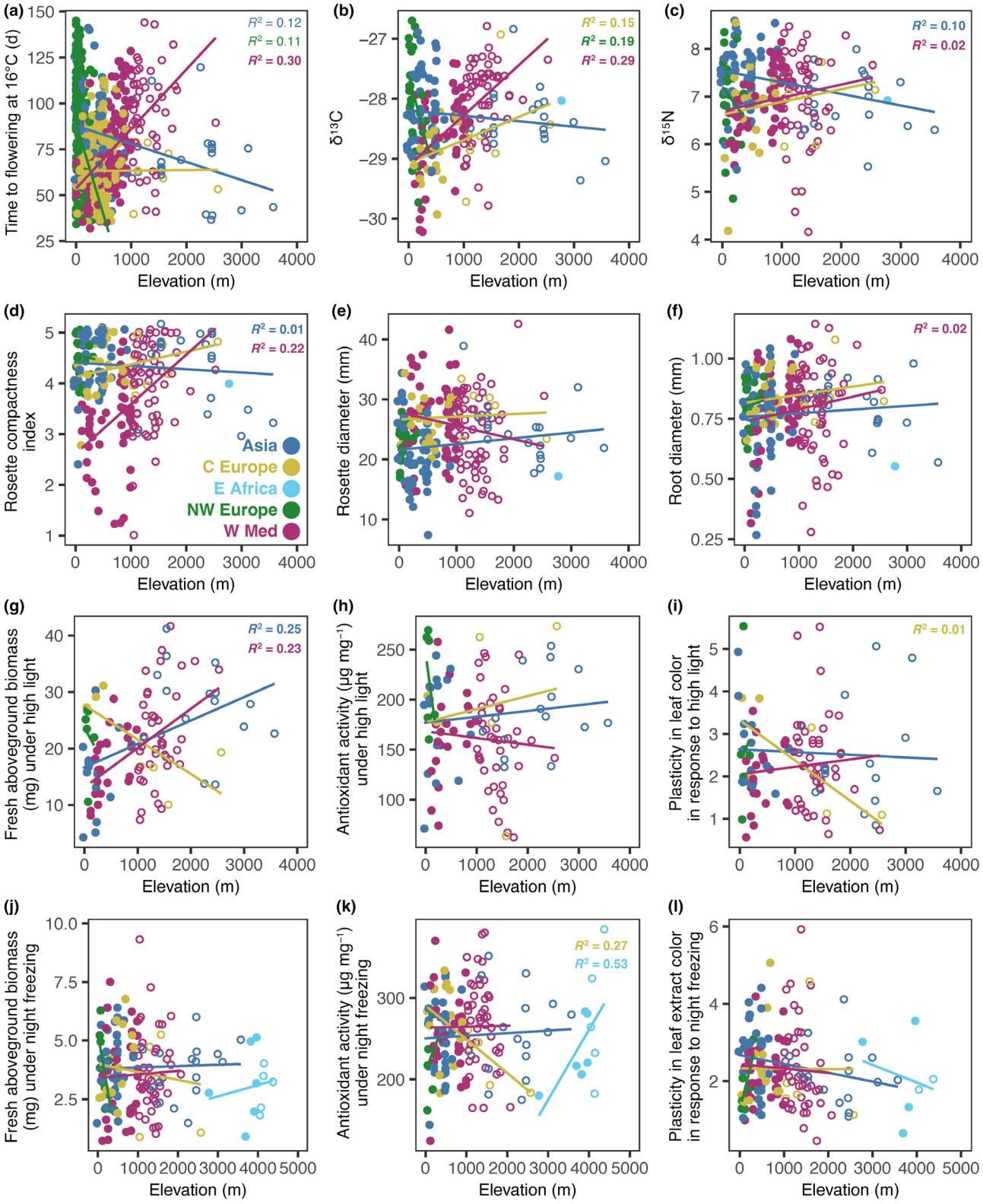

Fig. 3 Linear regressions on elevation of origin of *Arabidopsis thaliana* flowering time and phenotypes in three experiments simulating alpine stress. Points are ecotypes below (closed circles) and above (open circles) 1000 m above sea level, except for eastern Africa where the threshold is 4000 m. Ecotypes and fitted lines are colored by region with the legend displayed in (d). Trait–elevation plots are: (a) flowering time for plants grown under 16°C, (b–f) phenotypes grown under low CO_2 partial pressure, (g–i) phenotypes grown under high light, and (j–l) phenotypes grown under night freezing. Significant relationships ($P < 0.05$) are depicted by their R^2, and bolded when a model that accounted for kinship among ecotypes was also significant.

Table 1 Candidate genes mapped with genome-wide association studies for global and regional datasets of *Arabidopsis thaliana*.

Locus	Gene	Function	CHR	Coord (bp)	Strand	SNP (bp)	FDR	Phenotype	Region
AT4G00370	*PHT4;4*	Ascorbate transporter	4	162 897–166 357	(−)	160 735 162 202	0.001	HL Trolox	Global
AT5G49730	*FRO6*	Iron transporter	5	20 201 037–20 204 595	(−)	20 206 030	0.001	HL Trolox	Global
AT5G49740	*FRO7*	Iron transporter	5	20 205 302–20 208 777	(−)	20 206 030	0.001	HL Trolox	Global
AT5G45830	*DOG1*	Seed dormancy cold response	5	18 589 438–18 591 506	(−)	18 590 591 18 590 247	0.005 0.005	FT 16°C	W Med
AT5G23220	*NIC3*	Abscisic acid signaling	5	7819 608–7820 760	(−)	7818 730	0.02	$\delta^{13}C$	W Med
AT5G11850	*MAP3k*	Abscisic acid signaling	5	3816 080–3821 170	(−)	3821 491	0.09	$\delta^{13}C$	W Med
AT5G10150	*FLC*	Flowering time cold response	5	3181 938–3184 110	(−)	3177 182 3180 228	0.3 0.3	FT 16°C	Asia
AT1G64080	*MAKR2*	Auxin regulation in roots	1	23 784 977–23 786 800	(−)	23 791 370	0.006	$\delta^{13}C$	Asia
AT1G22550	*NPF5.16*	Vacuolar nitrate transport	1	7966 500–7968 692	(−)	7969 709	0.03	$\delta^{13}C$	Asia

CHR, chromosome; Coord, genomic coordinates in base pairs (bp); (−), DNA reverse strand; FT, flowering time; HL Trolox, antioxidant activity under high light (under cool temperature); W Med, western Mediterranean. The false discovery rate (FDR) was applied to gemma Wald test *P*-values.

$r = -0.2$, $P = 0.01$ chr5: 20206030 bp and *FRO7*). Accordingly, top GWAS genes ($n = 238$) were enriched for genes that compose the chloroplast membrane (5 genes, $P = 0.04$).

In western Mediterranean ecotypes, we mapped two QTL for $\delta^{13}C$ (FDR = 0.02 and 0.09) and one QTL for flowering time (FDR = 0.005). For $\delta^{13}C$, the top QTL (composed of 9 SNPs) and the fifth top QTL (composed of 3 SNPs) were adjacent (downstream and upstream, respectively) of two genes involved in abscisic acid (ABA) regulation under osmotic stress. The top was *NICOTINAMIDASE 3* (*NIC3*; AT5G23220), which encodes an enzyme that prevents the accumulation of intracellular nicotinamide by converting it into nicotinic acid in the NAD+ pathway, and which is expressed via Repressor of Silencing 1 (ROS1) DNA demethylation in response to ABA (Kim *et al.*, 2019). The other was *MAP3 kinase* (*MAP3k*; AT5G11850), which participates in the phosphorylation of SnRK2 kinases that in turn trigger osmotic stress and ABA responses (Takahashi *et al.*, 2020). Top $\delta^{13}C$ GWAS genes ($n = 205$) were enriched for genes involved in cellular response to ABA stimulus (five genes, $P = 0.02$). For flowering time, the top QTL (composed of 47 SNPs) was in and around *DELAY OF GERMINATION 1* (*DOG1*; AT5G45830), an extensively studied gene involved in regulating seed dormancy and perhaps also flowering time (Graeber *et al.*, 2014; Huo *et al.*, 2016; Martínez-Berdeja *et al.*, 2020). Top flowering time GWAS genes ($n = 127$) were enriched for genes involved in response to ABA (6 genes, $P = 0.03$).

In Asian ecotypes, we mapped two QTL for $\delta^{13}C$ (FDR = 0.006 and 0.03), and one QTL for flowering time (but FDR = 0.3). For $\delta^{13}C$, the top QTL (composed of 9 SNPs) was upstream of *MEMBRANE-ASSOCIATED KINASE REGULATOR 2* (*MAKR2*; AT1G64080), a receptor-like kinase that is involved in auxin regulation during root gravitropism (Marquès-Bueno *et al.*, 2021). The second top QTL (composed of 1 SNP) was a Major facilitator superfamily protein (*NPF5.16*; AT1G22550) involved in vacuolar nitrate transmembrane transport that likely functions under osmotic stress (Lu *et al.*, 2022). Top $\delta^{13}C$ GWAS genes ($n = 156$) were enriched for genes involved in response to osmotic stress (7 genes, $P = 0.04$). For flowering time, the 20th top QTL (composed of 19 SNPs) was upstream of *FLOWERING LOCUS C* (*FLC*; AT5G10150). *FLC* is a flowering repressor and is downregulated through epigenetic silencing induced by vernalization, *FRIGIDA*, or *VERNALIZATION INSENSITIVE 3* (Hepworth *et al.*, 2020). Late flowering alleles were almost restricted to the Caucasus (AF in Asia = 0.18–0.21, AF in Caucasus = 0.49–0.54), but unrelated to elevation despite the observed trend of earlier flowering at higher elevations. Also, late flowering alleles were present in both Caucasus genetic clusters, suggesting admixture or shared ancestral variation. Top flowering time GWAS genes ($n = 163$) were enriched for genes involved in defense response (14 genes, $P = 0.03$).

Putative QTL showed elevational clines in respective regions

We detected significant allele frequency–elevation clines in regional QTL with linear mixed kinship models (Figs 4, 5). In western Mediterranean ecotypes, alleles associated with late flowering and high $\delta^{13}C$ were frequent at high elevation ($P = 7 \times 10^{-6}$ for chr5: 18590591 bp/*DOG1* and $P = 0.02$ for chr5: 7818730 bp/*NIC3*, but $P = 0.07$ for chr5: 3821491 bp/*MAP3k*), suggesting changing selection with elevation on these genes contributes to elevational clines in phenology and in $\delta^{13}C$ via ABA signaling and stomatal dynamics. In Iberia, alleles associated with low $\delta^{13}C$/rapid flowering occurred in coastal and lowland areas with late-spring heat and drought in various mountains, except where the minor allele was rare or absent (Fig. 4a–i).

In Asia, QTL-elevation clines varied depending on the mountain range. In central Asia, alleles involved in high $\delta^{13}C$ were frequent at low elevations ($P = 9 \times 10^{-8}$ for chr1: 23791370 bp/*MAKR2* and $P = 7.5 \times 10^{-8}$ for chr1: 7969709 bp/*NPF5.16*), suggesting that changing selection with elevation on those genes contributes to elevational clines in $\delta^{13}C$ via auxin and vacuolar nitrate dynamics, which are important for osmotic regulation (Naser & Shani, 2016; Lu *et al.*, 2022). Although these SNPs were not found among the top 100 in our flowering time GWAS, the high $\delta^{13}C$ variants in

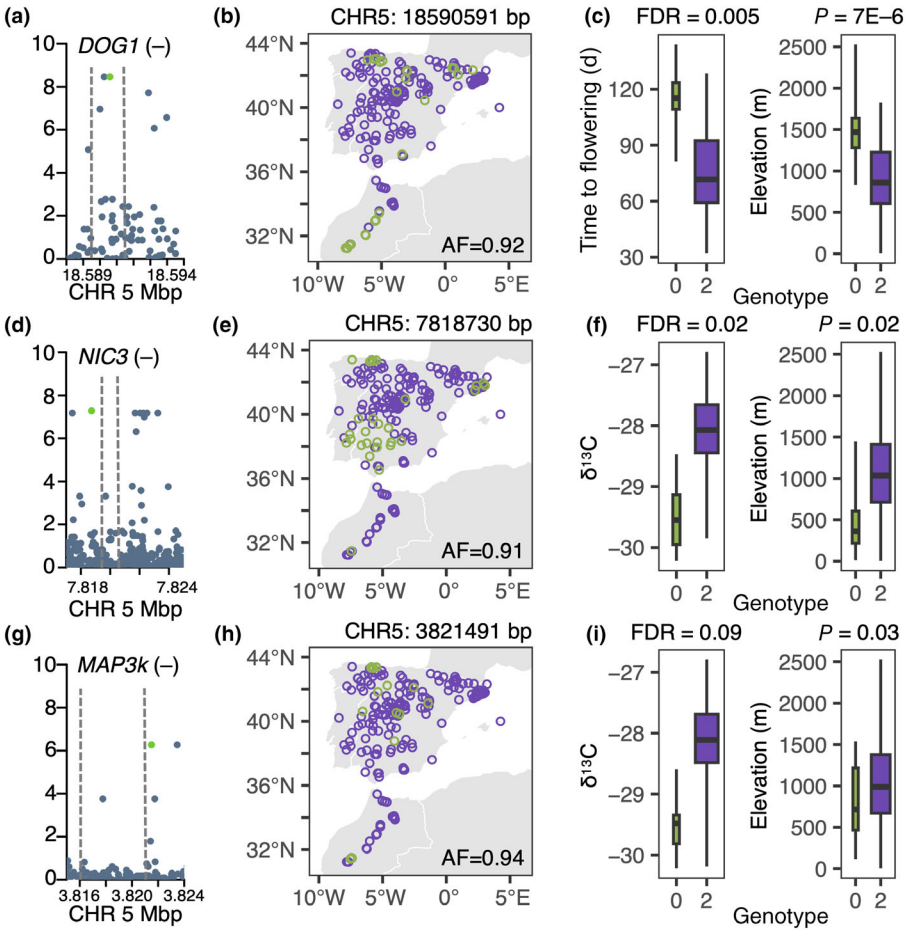

Fig. 4 *Arabidopsis thaliana* quantitative trait loci (QTL) mapped in the western Mediterranean with genome-wide association studies (GWAS), showing geographic distribution, effect size, and elevational variation of top single-nucleotide polymorphism (SNP) of flowering time QTL (top panels), and δ^{13}C QTL (middle and bottom panels). (a, d, g) Manhattan plots zoomed-in on candidate gene QTL (surrounded by dashed lines), showing their orientation (+, forward; −, reverse) and associated SNPs marked in green. SNPs were filtered for MAF < 0.05: n = 183 ecotypes and 2653 237 SNPs for flowering time, and n = 110 ecotypes and 2831 054 for δ^{13}C. (b, e, h) Map of top SNP QTL in the western Mediterranean with colors distinguishing SNP alleles (0, alternate allele; 2, reference allele in boxplots). (c, f, i) Variation of GWAS SNP alleles relative to traits (left, with GWAS FDR), and elevation (right, with P-value from a kinship mixed model). Boxplot width is proportional to allele frequency (AF) and depicts the median and interquartile range, with whiskers extending to the data extremes.

central Asia were significantly associated with delayed flowering ($P = 8 \times 10^{-6}$ for chr1: 23791370 bp/*MAKR2* and $P = 1.4 \times 10^{-5}$ for chr1: 7969709 bp/*NPF5.16*). In the Caucasus, only chr1: 23791370 bp/*MAKR2* showed an elevational trend, with the high δ^{13}C allele mostly found at high elevations ($P = 0.06$), but that SNP showed no association to flowering time ($P = 0.3$). Lastly, the *FLC* early flowering variants (in chr5: 3177182 bp and 3180 228 bp) were almost restricted to the Caucasus and tended to occur at higher elevation, but associations were weak and not significant when accounting for kinship among ecotypes ($P > 0.75$; Fig. 5a–i).

DOG1 haplotypes showed repeated regional trends in flowering time, but not in elevation

The *DOG1* SNP (chr5: 18590591 bp) found in the western Mediterranean was previously identified by Martínez-Berdeja *et al.* (2020) because of its association with seed dormancy in response to cold. The late flowering allele tags some (15 of 52 in Iberia and 15 of 68 in Morocco) of the ecotypes carrying the widespread ancestral haplotype of the *DOG1* self-binding domain (ECCY), but this SNP did not segregate in ecotypes with other haplotypes. Delayed flowering was more frequent in ECCY ecotypes in all regions (Kruskal–Wallis $P < 0.005$; Fig. S6a). ECCY ecotypes behave as winter annuals: seeds germinate soon after dispersal in the late summer–early fall (if not, extended cold induces secondary dormancy), plants overwinter as small rosettes, and flower over the spring (Martínez-Berdeja *et al.*, 2020).

Martínez-Berdeja *et al.* (2020) noted some global climatic pattern in the distribution of *DOG1* haplotypes but did not characterize the direction of elevational clines. We found that *DOG1* haplotype frequency significantly changes with elevation in western Mediterranean and northwestern Europe ecotypes (Kruskal–Wallis $P < 0.0005$), but not in Asia or central Europe ($P > 0.1$; Fig. S6b). Relative to other haplotypes, ECCY was associated with higher elevations in the western Mediterranean, but with lower elevations in northwestern Europe. Thus, the role of *DOG1* in local adaptation along elevation likely differs from region to region due to alternate life-history clines among regions.

The spatial scale of trait and QTL-elevational clines followed the extent of different mountainous regions

To characterize the spatial turnover in trait–elevation clines, we focused on flowering time and δ^{13}C, two of the traits thought to be most important in local adaptation to different conditions. For these traits, GAMs with spatially varying coefficients identified northwest Spain (Galicia) as a center for the strongest positive cline and southern Siberia (Altai Krai) as a center for the strongest negative cline (Fig. S7). We then recalculated these

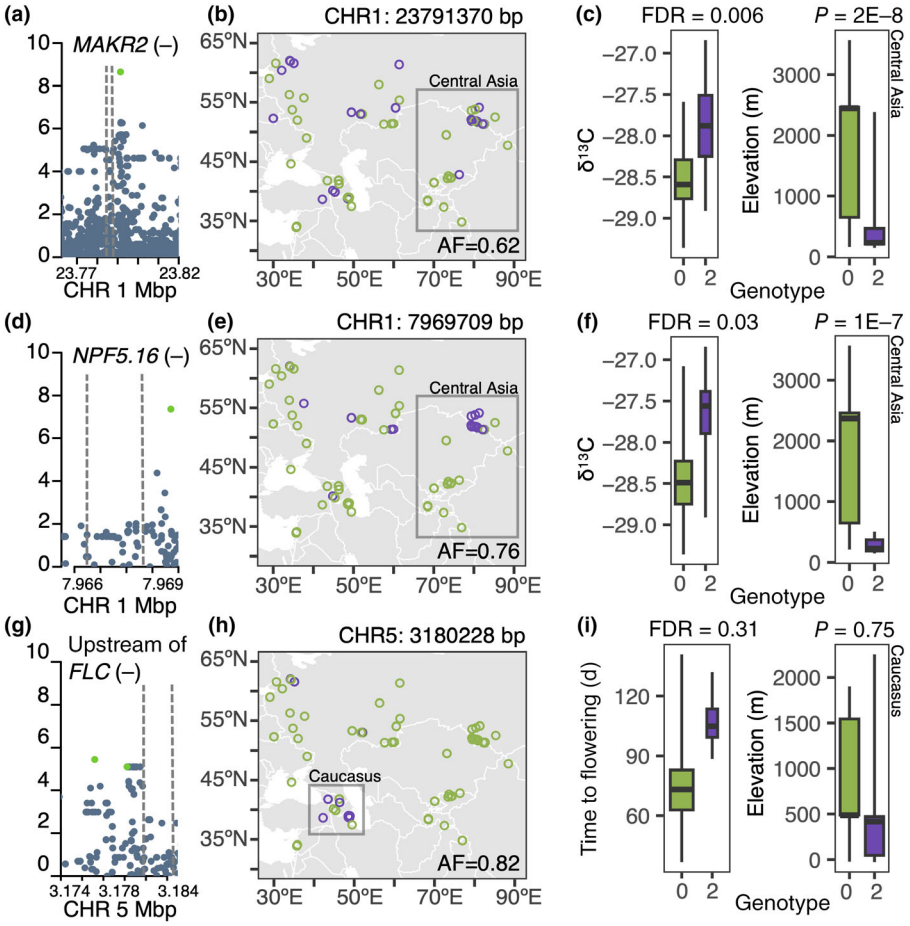

Fig. 5 *Arabidopsis thaliana* quantitative trait loci (QTL) mapped in Asia with genome-wide association studies (GWAS), showing geographic distribution, effect size, and elevational variation of top single-nucleotide polymorphism (SNP) of δ^{13}C QTL (top and middle panels) and flowering time QTL (bottom panel). (a, d, g) Manhattan plots zoomed-in on candidate gene QTL (surrounded by dashed lines), showing their orientation (+, forward; −, reverse) and associated SNPs marked in green. SNPs were filtered for MAF < 0.05: n = 76 ecotypes and 2572 318 SNPs for δ^{13}C, and n = 110 ecotypes and 2514 021 for flowering time. (b, e, h) Map of top SNP QTL in Asia with colors distinguishing SNP alleles (0, alternate allele; 2, reference allele in boxplots) and gray boxes showing subregions where SNPs show elevation turnover. (c, f, i) Variation of GWAS SNP alleles relative to traits (left, with GWAS FDR), and elevation (right, with P-value from a kinship mixed model using ecotypes in map gray boxes). Boxplot width is proportional to allele frequency (AF) and depicts the median and interquartile range, with whiskers extending to the data extremes.

clines within regions of expanding radii centering our analyses separately at these two opposite ends of the Arabidopsis distribution. For analysis centered on the location of a Galician ecotype, strong positive flowering time and δ^{13}C clines with elevation ($r \sim 0.5$) are maintained until *c.* 2000 km distance, beyond which distance the inclusion of Scandinavian ecotypes with different relationships weaken the clines. Centering the analysis on Altai Krai, strong negative clines ($r \sim -0.5$) in these traits are maintained up to nearly 3000 km (and further for flowering time), beyond which distance the inclusion of eastern European and Mediterranean ecotypes weaken the clines.

As our sample size was greater in the western Mediterranean, we used the top flowering time and δ^{13}C SNPs to analyze the spatial scale at which elevational clines change, given that these traits showed opposing clines in other regions. We found remarkably similar change in allele frequency clines with greater distances from Spain compared with the change in trait clines for which these loci were QTL (Fig. 6a–d).

Climate gradients associated with elevational allele frequency clines changed between regions

In the western Mediterranean, when testing the correlation of GWAS SNPs with bioclimatic variables, we found that both the *DOG1* and *NIC3* SNP alleles were most strongly associated with variation in the minimum temperature of the coldest month (gemma Wald test P = 0.004 for *DOG1* and P = 0.0003 for *NIC3*). By contrast, the *MAP3k* SNP was most strongly associated with temperature seasonality (P = 0.009). In these three cases, the high-elevation allele was associated with colder winter temperatures or greater temperature seasonality. When testing for enrichment of the top 1000 SNPs for these traits, we found δ^{13}C SNPs were most enriched for strong associations with minimum temperature of the coldest month (permutation $P < 0.01$, fifth percentile of P-values for climate association $< 10^{-5}$) and flowering time was most enriched for strong associations with mean temperature of coldest quarter ($P < 0.01$, fifth percentile of P-values for climate association = 0.007). These QTL were not enriched in associations with precipitation variables (Table S3).

In Asia, when testing the correlation of GWAS SNPs with bioclimatic variables, we found the *MAKR2* SNP was most strongly associated with temperature annual range (P = 0.0329) with the low δ^{13}C/low WUE allele associated with less annual range. The *NPF5.16* SNP was most strongly associated with temperature seasonality (P = 0.0018) with the low WUE allele associated with low seasonality. The *FLC* SNP chr5: 3177182 was most strongly associated with mean temperature of the driest quarter (P = 0.0002) with the early flowering allele associated with cooler driest quarters. Chr5: 3180228 was most strongly associated with precipitation of warmest quarter (P = 0.0051) with early flowering allele associated

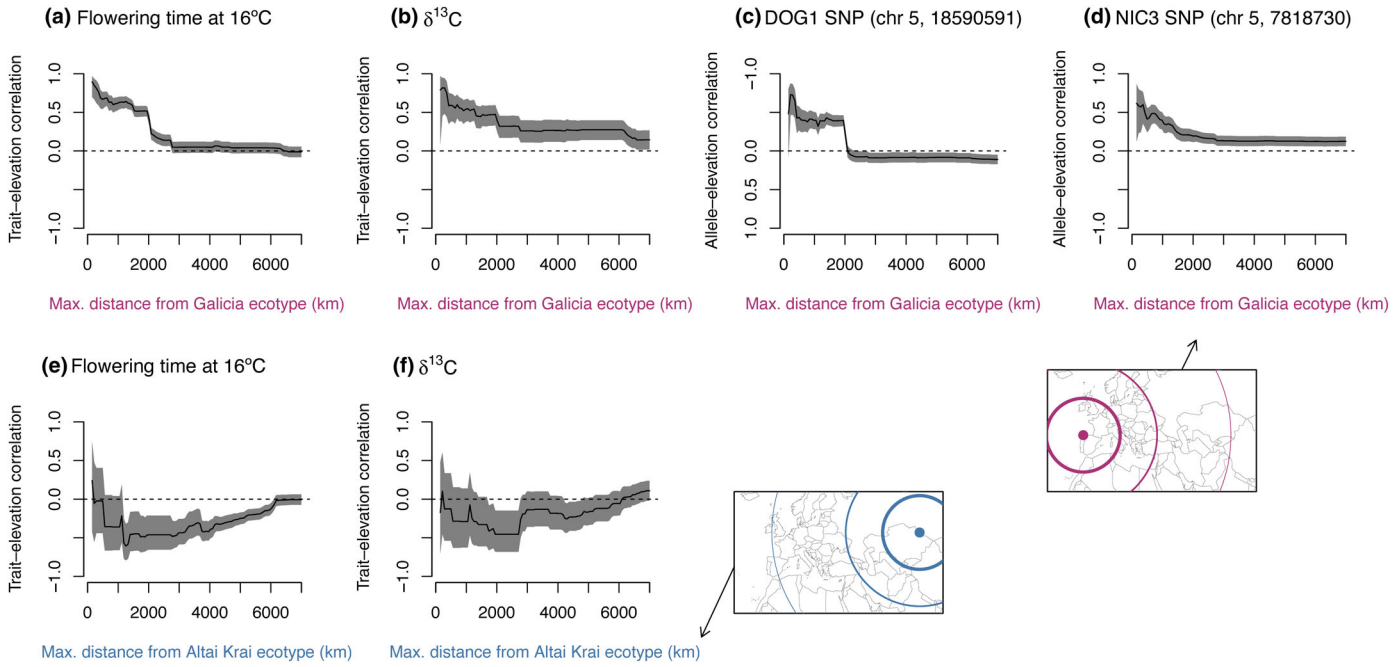

Fig. 6 Spatial scale of *Arabidopsis thaliana* regional elevational clines, *that is* of the trait–elevation and corresponding quantitative trait loci (QTL) allele frequency–elevation correlation. Upper panels correspond to the western Mediterranean (a–d) and lower panels correspond to Asia (e, f). Elevational clines are centered at locations with particularly strong correlations: Galicia in the western Mediterranean shows strong positive correlations and Altai Kai in Asia shows strong negative correlations. Shaded regions demark 95% CIs of Pearson correlation coefficients. QTL allele frequency–elevation clines were not evaluated in Asia due to small sample size.

with wetter warmest quarters. When testing for enrichment of the top 1000 SNPs for these traits, we found $\delta^{13}C$ SNPs were most enriched for strong associations with temperature seasonality (permutation $P < 0.01$, fifth percentile of P-values for climate association $= 1.6 \times 10^{-5}$). Flowering time SNPs were most enriched for strong associations with precipitation of the warmest quarter (permutation $P < 0.01$, fifth percentile of P-values for climate association = 0.0051; Table S4).

Discussion

Arabidopsis exhibits natural genetic variation in adaptive traits, which may be linked to changing selection along elevational gradients. Germination and flowering time show evidence of local adaptation in response to seasonal cold at high elevations and to early drought at low elevations (Méndez-Vigo *et al.*, 2011; Suter *et al.*, 2014; Vidigal *et al.*, 2016). Water use efficiency and its genetic basis may be associated with phenology (Lovell *et al.*, 2013; Kenney *et al.*, 2014), though changes in WUE with elevation are less clear (Mckay *et al.*, 2003; Des Marais *et al.*, 2014; Wolfe & Tonsor, 2014; Dittberner *et al.*, 2018; DeLeo *et al.*, 2020). Past studies have typically focused on individual regions in Eurasia and rarely included Africa, precluding a broader understanding of adaptation to global elevational gradients (Tyagi *et al.*, 2016; Tripathi *et al.*, 2019).

We examined the regional heterogeneity of selection associated with elevational gradients in Arabidopsis, by integrating whole-genomes, alpine stress phenotypes, and life cycle. By accounting for genome-wide patterns of variation among ecotypes, we uncovered elevational clines indicating changing selection on several traits and genomic variants. Most clines were region-specific and likely part of a coordinated phenology-physiology strategy. Despite similarities in elevation–environment gradients among separate mountain ranges, we showed that patterns of multivariate selection associated with elevation and their genetic basis can be unique to each region (Tusiime *et al.*, 2020; Wos *et al.*, 2022). This is likely due to global genetic heterogeneity (*sensu* López-Arboleda *et al.*, 2021) affected by differences in selective environmental regimes among regions, that result in unique phenotypic clines. Additionally, selfing and limited dispersal in Arabidopsis could promote a mosaic of locally adaptive polymorphisms that are globally rare but locally abundant (Brachi *et al.*, 2013; Horton *et al.*, 2016; Gould & Stinchcombe, 2017). Alternatively, global polymorphisms could be under selection only in certain populations (Lee & Coop, 2019).

Genetic heterogeneity in Arabidopsis elevational clines

Population genetic patterns mostly suggest relatively high gene flow between nearby high and low elevations because nearby populations are usually related, and elevation plays a weak role in explaining population structure (except in the Caucasus). Greater gene flow among sites with similar elevations and environmental conditions could increase the chances of shared genetic

mechanisms of local adaptation (Stuart *et al.*, 2017; Wos *et al.*, 2022). However, Arabidopsis lacks mechanisms for long-distance pollen and seed dispersal, resulting in limited gene flow that is not able to counteract the effect of drift in populations, consistent with isolation-by-distance being the greater determinant of population structure compared with isolation-by-environment along elevational gradients. The substantial genetic differences among similar alpine habitats in distant regions may thus contribute to heterogeneity in mechanisms of local adaptation to elevation (Bohutínská & Peichel, 2023).

The biogeographic history of Arabidopsis may have also favored evolution of distinct elevational clines. For example, the western Mediterranean and Asia were likely colonized during separate migrations, first from Africa during the last interglacial in Eurasia (*c.* 120–90 ka, *that is* 'relicts' expansion), and more recently from the Caucasus (*c.* 45 ka, *that is* Eurasian clade expansion) (Fulgione & Hancock, 2018). The position of these populations at opposite ends of the range, > 5000 km distant, likely reduced the amount of shared standing genetic variation available for elevational adaptation, promoting independent mechanisms of adaptation (Lee & Coop, 2019).

Potential drivers of heterogeneity in changes in selection along elevation gradients

The contrasting clines in life history and physiology among regions may be in some sense surprising given similar elevational trends in climate, though there were potentially important climatic differences among these regions. Western Mediterranean ecotypes inhabited milder temperatures with great variation in summer precipitation. By contrast, Asian ecotypes inhabited more seasonal temperatures with colder winters. Given such climatic differences, these two regions might harbor alternative strategies of elevational adaptation that are under different selection regimes.

In the western Mediterranean, previous studies support drought escape at low elevations and a more conservative, stress-avoiding winter-annual strategy at high elevations (e.g. Montesinos-Navarro *et al.*, 2011), though ecotypes with different strategies may coexist at the same elevation (Picó, 2012). Furthermore, genetic variation in *DOG1* gene expression and elevation were correlated in Iberia (Vidigal *et al.*, 2016). We show that flowering time and $\delta^{13}C$ QTL had significant allele frequency correlations with cold temperatures during the winter, suggesting that selection associated with cold partly drives elevational clines in this region (e.g. Tabas-Madrid *et al.*, 2018).

In Asia, adaptation to high elevation is less well documented, but may imply drought escape (our study), greater plasticity in flowering time (Singh & Roy, 2017), and/or a deletion in *FLC* associated with early flowering (Yang *et al.*, 2024) not detected in our GWAS. In general, the harsher temperatures in Asia may prohibit winter-annual strategies at the very coldest high-elevation sites and allow only more rapid cycling strategies. We found that flowering time and $\delta^{13}C$ QTL showed significant allele frequency correlations with summer precipitation and temperature seasonality, suggesting that selection by these gradients could drive elevational clines in this region.

Coordinated life cycle and physiology along elevation

The opposite clines we described in the Iberian and Central Asian mountains involved a correlation of late flowering and higher WUE. Previous studies have found genetic correlations between high WUE and late flowering due to variation across the genome (Kenney *et al.*, 2014) and specifically to pleiotropic effects of a flowering time regulator (*FRI*), that affects expression of *FLC* (Lovell *et al.*, 2013). Our results suggest that genetic correlations between WUE and flowering time involves variation in other genes. In the western Mediterranean, there could be interactions between the seed dormancy regulator *DOG1* (Martínez-Berdeja *et al.*, 2020) and ABA signaling genes. In Central Asia, the genetic basis of flowering time variation was unclear but flowering time was correlated with allele frequency of $\delta^{13}C$ QTL, suggesting a potential pleiotropic effect of phenology and physiological regulation. Testing these hypotheses will require detailed experiments with crosses or knockouts.

Traits associated with protection from photooxidation

Ecotypes showed increases in antioxidants and changes in leaf color in response to bright light and night freezing, but little associations with elevation. Photooxidation may also be a threat at lower elevations due to drought, potentially resulting in no clear change in selection from low elevations where drought is common to high elevation where cold is common (Nakabayashi *et al.*, 2014). Furthermore, while changes in antioxidants and pigments mediate high light acclimation (Aarabi *et al.*, 2023), antioxidants alone might not indicate freezing tolerance (Distelbarth *et al.*, 2013, but see Hannah *et al.*, 2006). The combination of cold and high light can thus comprise diverse metabolic and genomic pathways, that could be region-specific, and which detection requires denser regional sampling.

Afroalpine ecotypes occupy an outlier environment with respect to clear sky radiation and night-cold throughout the year. There we found that antioxidant activity under night freezing tended to increase with elevation. Also, darker leaf extracts were associated with higher survival rates. These results suggest cold acclimation involves antioxidants and pigments, but given our limited sampling in this region, this hypothesis needs additional testing.

Conclusions

Heterogeneity in the mechanisms of local adaptation may challenge global correlative studies in widespread species that link environment to genotype and phenotype (e.g. genotype–environment associations, Lasky *et al.*, 2023). By taking a global but multi-regional view of selection associated with elevation, we were able to identify such heterogeneity and its spatial patterns. This heterogeneity reinforces the value of regional diversity studies (e.g. Gloss *et al.*, 2022), where the power to dissect trait

evolution may be greater due to consistent mechanisms. Integrating regional patterns of plant adaptation at a range-wide scale may help improve evolutionary predictions for globally important plants under anthropogenic global change.

Acknowledgements

We thank Xavier Picó and four anonymous reviewers for their comments on earlier versions of this manuscript. Plant material was exported from Uganda with permission of The Ministry of Agriculture, Animal Industry and Fisheries' Plant Quarantine and Inspection Services, permit UQIS 4414/93/PC (E). Material was exported from Ethiopia with permission of the Ethiopian Biodiversity Institute (ref. no.: EBE71/7065/2018). Material was imported to the USA under USDA APHIS permits P37-17-01651 and P37-18-00230. Amanda Penn, Chloee McLaughlin, Jeremy Sutherland, Tim Gilpatrick, Connor Campana, Victoria Meagher, and Jaden Hill assisted in the experiment setup and rosette harvests. Shawn Burghard advised in pest and disease control. Ken Long assisted with growth chamber operation and maintenance. Funding was provided by NSF DEB-1927009 and NIH R35GM138300 awards to JRL.

Competing interests

None declared.

Author contributions

DG, CML and JRL designed the research. DG, CML, AH, SS, LL, TX, MT, EK, DE, JK, MY, CE, and TW performed research. DG, CML, SS, LL, TX, MT and EK analyzed data. DG, CML, SS, KG and JRL wrote the paper with the contributions of all other authors.

ORCID

Collins E. Bulafu https://orcid.org/0000-0002-1008-3634
Dinakaran Elango https://orcid.org/0000-0003-2226-486X
Diana Gamba https://orcid.org/0000-0002-0421-6437
Katarzyna Glowacka https://orcid.org/0000-0002-8892-1482
Jeffrey Kerby https://orcid.org/0000-0002-2739-9096
Evelyn Kulesza https://orcid.org/0000-0002-5619-9317
Jesse R. Lasky https://orcid.org/0000-0001-7688-5296
Lua Lopez https://orcid.org/0000-0002-3619-763X
Seema Sahay https://orcid.org/0000-0001-5707-2206
Margarita Takou https://orcid.org/0000-0001-6176-6251
Tigist Wondimu https://orcid.org/0000-0003-2212-3362
Mistire Yifru https://orcid.org/0000-0001-7113-8347

Data availability

The data that support the findings of this study are available in the supplementary material of this article (Datasets S2, S6). New sequences are available in the European Nucleotide Archive (ENA; https://www.ebi.ac.uk/ena) under project PRJEB79562 (accession nos.: ERS20926326–ERS20926335). Processed sequence data (bam files), a VCF with newly sequenced eastern Africa ecotypes, and raw phenotype data are available in the Figshare public repository with DOI: 10.6084/m9.figshare.23960727.

References

Aarabi F, Ghigi A, Ahchige MW, Bulut M, Geigenberger P, Neuhaus HE, Sampathkumar A, Alseekh S, Fernie AR. 2023. Genome-wide association study unveils ascorbate regulation by *PAS/LOV PROTEIN* during high light acclimation. *Plant Physiology* **193**: 2037–2054.

Abbas M, Sharma G, Dambire C, Marquez J, Alonso-Blanco C, Proaño K, Holdsworth MJ. 2022. An oxygen-sensing mechanism for angiosperm adaptation to altitude. *Nature* **606**: 565–571.

Alonso-Blanco C, 1001 Genomes Consortium. 2016. 1,135 genomes reveal the global pattern of polymorphism in *Arabidopsis thaliana*. *Cell* **166**: 481–491.

Bohutínská M, Peichel CL. 2023. Divergence time shapes gene reuse during repeated adaptation. *Trends in Ecology & Evolution* **39**: 396–407.

Bohutínská M, Vlček J, Yair S, Laenen B, Konečná V, Fracassetti M, Slotte T, Kolář F. 2021. Genomic basis of parallel adaptation varies with divergence in *Arabidopsis* and its relatives. *Proceedings of the National Academy of Sciences, USA* **118**: e2022713118.

Brachi B, Villoutreix R, Faure N, Hautekèete N, Piquot Y, Pauwels M, Roby D, Cuguen J, Bergelson J, Roux F. 2013. Investigation of the geographical scale of adaptive phenological variation and its underlying genetics in *Arabidopsis thaliana*. *Molecular Ecology* **22**: 4222–4240.

Brennan AC, Méndez-Vigo B, Haddioui A, Martínez-Zapater JM, Picó FX, Alonso-Blanco C. 2014. The genetic structure of *Arabidopsis thaliana* in the south-western Mediterranean range reveals a shared history between North Africa and southern Europe. *BMC Plant Biology* **14**: 17.

Brochmann C, Gizaw A, Chala D, Kandziora M, Eilu G, Popp M, Pirie MD, Gehrke B. 2021. History and evolution of the Afroalpine flora: in the footsteps of Olov Hedberg. *Alpine Botany* **132**: 65–87.

Caldas FJ. 1966. *Obras completas de Francisco José de Caldas: publicadas por la Universidad Nacional de Colombia como homenaje con motivo del sesquicentenario de su muerte*. Bogotá, Colombia: Imprenta Nacional.

Cheng CY, Krishnakumar V, Chan AP, Thibaud-Nissen F, Schobel S, Town CD. 2017. Araport11: a complete reannotation of the *Arabidopsis thaliana* reference genome. *The Plant Journal* **89**: 789–804.

Clarke RT, Rothery P, Raybould AF. 2002. Confidence limits for regression relationships between distance matrices: estimating gene flow with distance. *JABES* **7**: 361–372.

Clausen J, Keck DD, Hiesey WM. 1940. Experimental studies on the nature of species. I. Effect of varied environments on western North American plants. *Madroño: A West American Journal of Botany* **6**: 60–63.

DeLeo VL, Menge DNL, Hanks EM, Juenger TE, Lasky JR. 2020. Effects of two centuries of global environmental variation on phenology and physiology of *Arabidopsis thaliana*. *Global Change Biology* **26**: 523–538.

Des Marais DL, Auchincloss LC, Sukamtoh E, McKay JK, Logan T, Richards JH, Juenger TE. 2014. Variation in *MPK12* affects water use efficiency in Arabidopsis and reveals a pleiotropic link between guard cell size and ABA response. *Proceedings of the National Academy of Sciences, USA* **111**: 2836–2841.

Distelbarth H, Nägele T, Heyer AG. 2013. Responses of antioxidant enzymes to cold and high light are not correlated to freezing tolerance in natural accessions of *Arabidopsis thaliana*. *Plant Biology Journal* **15**: 982–990.

Dittberner H, Korte A, Mettler-Altmann T, Weber APM, Monroe G, de Meaux J. 2018. Natural variation in stomata size contributes to the local adaptation of water-use efficiency in *Arabidopsis thaliana*. *Molecular Ecology* **27**: 4052–4065.

Durvasula A, Fulgione A, Gutaker RM, Alacakaptan SI, Flood PJ, Neto C, Tsuchimatsu T, Burbano HA, Picó FX, Alonso-Blanco C *et al.* 2017. African genomes illuminate the early history and transition to selfing in *Arabidopsis thaliana*. *Proceedings of the National Academy of Sciences, USA* **114**: 5213–5218.

Feng H, An F, Zhang S, Ji Z, Ling HL, Zuo J. 2006. Light-regulated, tissue-specific, and cell differentiation-specific expression of the *Arabidopsis* Fe(III)-chelate reductase gene AtFRO6. *Plant Physiology* **140**: 1345–1354.

Fernández-Marín B, Gulías J, Figueroa CM, Iñiguez C, Clemente-Moreno MJ, Nunes-Nesi A, Fernie AR, Cavieres LA, Bravo LA, García-Plazaola JI *et al.* 2020. How do vascular plants perform photosynthesis in extreme environments? An integrative ecophysiological and biochemical story. *The Plant Journal* **101**: 979–1000.

Fulgione A, Hancock AM. 2018. Archaic lineages broaden our view on the history of *Arabidopsis thaliana*. *New Phytologist* **219**: 1194–1198.

Gloss AD, Vergnol A, Morton TC, Laurin PJ, Roux F, Bergelson J. 2022. Genome-wide association mapping within a local *Arabidopsis thaliana* population more fully reveals the genetic architecture for defensive metabolite diversity. *Philosophical Transactions of the Royal Society B: Biological Sciences* **377**: 20200512.

Gould BA, Stinchcombe JR. 2017. Population genomic scans suggest novel genes underlie convergent flowering time evolution in the introduced range of *Arabidopsis thaliana*. *Molecular Ecology* **26**: 92–106.

Graeber K, Linkies A, Steinbrecher T, Mummenhoff K, Tarkowská D, Turečková V, Ignatz M, Sperber K, Voegele A, De Jong H *et al.* 2014. *DELAY OF GERMINATION 1* mediates a conserved coat-dormancy mechanism for the temperature- and gibberellin-dependent control of seed germination. *Proceedings of the National Academy of Sciences, USA* **111**: E3571–E3580.

Günther T, Lampei C, Barilar I, Schmid KJ. 2016. Genomic and phenotypic differentiation of *Arabidopsis thaliana* along altitudinal gradients in the North Italian Alps. *Molecular Ecology* **25**: 3574–3592.

Gutaker RM, Groen SC, Bellis ES, Choi JY, Pires IS, Bocinsky RK, Slayton ER, Wilkins O, Castillo CC, Negrão S *et al.* 2020. Genomic history and ecology of the geographic spread of rice. *Nature Plants* **6**: 492–502.

Hancock AM, Brachi B, Faure N, Horton MW, Jarymowycz LB, Sperone FG, Toomajian C, Roux F, Bergelson J. 2011. Adaptation to climate across the *Arabidopsis thaliana* genome. *Science* **334**: 83–86.

Hannah MA, Wiese D, Freund S, Fiehn O, Heyer AG, Hincha DK. 2006. Natural genetic variation of freezing tolerance in *Arabidopsis*. *Plant Physiology* **142**: 98–112.

Havaux M, Kloppstech K. 2001. The protective functions of carotenoid and flavonoid pigments against excess visible radiation at chilling temperature investigated in *Arabidopsis* npq and tt mutants. *Planta* **213**: 953–966.

Hedberg I, Hedberg O. 1979. Tropical-alpine life-forms of vascular plants. *OIKOS* **33**: 297–307.

Hepworth J, Antoniou-Kourounioti RL, Berggren K, Selga C, Tudor EH, Yates B, Cox D, Collier Harris BR, Irwin JA, Howard M *et al.* 2020. Natural variation in autumn expression is the major adaptive determinant distinguishing *Arabidopsis FLC* haplotypes. *eLife* **9**: e57671.

Horton MW, Willems G, Sasaki E, Koornneef M, Nordborg M. 2016. The genetic architecture of freezing tolerance varies across the range of *Arabidopsis thaliana*. *Plant, Cell & Environment* **39**: 2570–2579.

Huo H, Wei S, Bradford KJ. 2016. DELAY OF GERMINATION1 (DOG1) regulates both seed dormancy and flowering time through microRNA pathways. *Proceedings of the National Academy of Sciences, USA* **113**: E2199–E2206.

Jain A, Wilson GT, Connolly EL. 2014. The diverse roles of *FRO* family metalloreductases in iron and copper homeostasis. *Frontiers in Plant Science* **5**: 100.

Jeong J, Cohu C, Kerkeb L, Pilon M, Connolly EL, Guerinot ML. 2008. Chloroplast Fe (III) chelate reductase activity is essential for seedling viability under iron limiting conditions. *Proceedings of the National Academy of Sciences, USA* **105**: 10619–10624.

Jeong J, Connolly EL. 2009. Iron uptake mechanisms in plants: functions of the *FRO* family of ferric reductases. *Plant Science* **176**: 709–714.

Karger DN, Conrad O, Böhner J, Kawohl T, Kreft H, Soria-Auza RW, Zimmermann NE, Linder HP, Kessler M. 2020. Climatologies at high resolution for the earth's land surface areas. *Scientific Data* **4**: 170122.

Kawakatsu T, Huang SSC, Jupe F, Sasaki E, Schmitz RJ, Urich MA, Castanon R, Nery JR, Barragan C, He Y *et al.* 2016. Epigenomic diversity in a global collection of *Arabidopsis thaliana* accessions. *Cell* **166**: 492–505.

Kenney AM, McKay JK, Richards JH, Juenger TE. 2014. Direct and indirect selection on flowering time, water-use efficiency (WUE, $\delta^{13}C$), and WUE plasticity to drought in *Arabidopsis thaliana*. *Ecology and Evolution* **4**: 4505–4521.

Kim JS, Lim JY, Shin H, Kim BG, Yoo SD, Kim WT, Huh JH. 2019. ROS1-dependent DNA demethylation is required for ABA-inducible *NIC3* expression. *Plant Physiology* **179**: 1810–1821.

Kooyers NJ, Greenlee AB, Colicchio JM, Oh M, Blackman BK. 2015. Replicate altitudinal clines reveal that evolutionary flexibility underlies adaptation to drought stress in annual *Mimulus guttatus*. *New Phytologist* **206**: 152–165.

Körner C. 2003. Ecological impacts of atmospheric CO_2 enrichment on terrestrial ecosystems. *Philosophical Transactions of the Royal Society A: Mathematical, Physical and Engineering Sciences* **361**: 2023–2041.

Körner C. 2007. The use of 'altitude' in ecological research. *Trends in Ecology & Evolution* **22**: 569–574.

Körner C. 2021. *Alpine plant life: functional plant ecology of high mountain ecosystems*. Berlin & Heidelberg, Germany: Springer Berlin & Heidelberg.

Lamesch P, Berardini TZ, Li D, Swarbreck D, Wilks C, Sasidharan R, Muller R, Dreher K, Alexander DL, Garcia-Hernandez M *et al.* 2012. The Arabidopsis Information Resource (TAIR): improved gene annotation and new tools. *Nucleic Acids Research* **40**: D1202–D1210.

Lampei C, Wunder J, Wilhalm T, Schmid KJ. 2019. Microclimate predicts frost hardiness of alpine *Arabidopsis thaliana* populations better than elevation. *Ecology and Evolution* **9**: 13017–13029.

Lasky JR, Des Marais DL, Lowry DB, Povolotskaya I, McKay JK, Richards JH, Keitt TH, Juenger TE. 2014. Natural variation in abiotic stress responsive gene expression and local adaptation to climate in *Arabidopsis thaliana*. *Molecular Biology and Evolution* **31**: 2283–2296.

Lasky JR, Josephs EB, Morris GP. 2023. Genotype–environment associations to reveal the molecular basis of environmental adaptation. *Plant Cell* **35**: 125–138.

Lee KM, Coop G. 2019. Population genomics perspectives on convergent adaptation. *Philosophical Transactions of the Royal Society B: Biological Sciences* **374**: 20180236.

López-Arboleda WA, Reinert S, Nordborg M. 2021. Global genetic heterogeneity in adaptive traits. *Molecular Biology and Evolution* **38**: 4822–4831.

Lovell JT, Juenger TE, Michaels SD, Lasky JR, Platt A, Richards JH, Yu X, Easlon HM, Sen S, McKay JK. 2013. Pleiotropy of *FRIGIDA* enhances the potential for multivariate adaptation. *Proceedings of the Royal Society Biological Sciences* **280**: 20131043.

Lu YT, Liu DF, Wen TT, Fang ZJ, Chen SY, Li H, Gong JM. 2022. Vacuolar nitrate efflux requires multiple functional redundant nitrate transporter in *Arabidopsis thaliana*. *Frontiers in Plant Science* **13**: 926809.

Luo Y, Widmer A, Karrenberg S. 2015. The roles of genetic drift and natural selection in quantitative trait divergence along an altitudinal gradient in *Arabidopsis thaliana*. *Heredity* **114**: 220–228.

Marquès-Bueno MM, Armengot L, Noack LC, Bareille J, Rodriguez L, Platre MP, Bayle V, Liu M, Opdenacker D, Vanneste S *et al.* 2021. Auxin-regulated reversible inhibition of *TMK1* signaling by *MAKR2* modulates the dynamics of root gravitropism. *Current Biology* **31**: 228–237.

Martínez-Berdeja A, Stitzer MC, Taylor MA, Okada M, Ezcurra E, Runcie DE, Schmitt J. 2020. Functional variants of *DOG1* control seed chilling responses and variation in seasonal life-history strategies in *Arabidopsis thaliana*. *Proceedings of the National Academy of Sciences, USA* **117**: 2526–2534.

Mckay JK, Richards JH, Mitchell-Olds T. 2003. Genetics of drought adaptation in *Arabidopsis thaliana*: I. Pleiotropy contributes to genetic correlations among ecological traits. *Molecular Ecology* **12**: 1137–1151.

Méndez-Vigo B, Picó FX, Ramiro M, Martínez-Zapater JM, Alonso-Blanco C. 2011. Altitudinal and climatic adaptation is mediated by flowering traits and *FRI, FLC*, and *PHYC* genes in *Arabidopsis*. *Plant Physiology* **157**: 1942–1955.

Miyaji T, Kuromori T, Takeuchi Y, Yamaji N, Yokosho K, Shimazawa A, Sugimoto E, Omote H, Ma JF, Shinozaki K *et al.* 2015. AtPHT4;4 is a chloroplast-localized ascorbate transporter in *Arabidopsis*. *Nature Communications* **6**: 5928.

Montesinos-Navarro A, Picó FX, Tonsor SJ. 2012. Clinal variation in seed traits influencing life cycle timing in *Arabidopsis thaliana*. *Evolution* **66**: 3417–3431.

Montesinos-Navarro A, Wig J, Picó FX, Tonsor SJ. 2011. *Arabidopsis thaliana* populations show clinal variation in a climatic gradient associated with altitude. *New Phytologist* **189**: 282–294.

Nakabayashi R, Yonekura-Sakakibara K, Urano K, Suzuki M, Yamada Y, Nishizawa T, Matsuda F, Kojima M, Sakakibara H, Shinozaki K *et al.* 2014. Enhancement of oxidative and drought tolerance in *Arabidopsis* by overaccumulation of antioxidant flavonoids. *The Plant Journal* **77**: 367–379.

Naser V, Shani E. 2016. Auxin response under osmotic stress. *Plant Molecular Biology* **91**: 661–672.

Paradis E, Claude J, Strimmer K. 2004. APE: analyses of phylogenetics and evolution in R language. *Bioinformatics* **20**: 289–290.

Peterman WP. 2018. ResistanceGA: an R package for the optimization of resistance surfaces using genetic algorithms. *Methods in Ecology and Evolution* **9**: 1638–1647.

Picó FX. 2012. Demographic fate of *Arabidopsis thaliana* cohorts of autumn- and spring-germinated plants along an altitudinal gradient. *Journal of Ecology* **100**: 1009–1018.

Poore HA, Stuart YE, Rennison DJ, Roesti M, Hendry AP, Bolnick DI, Peichel CL. 2023. Repeated genetic divergence plays a minor role in repeated phenotypic divergence of lake-stream stickleback. *Evolution* **77**: 110–122.

Singh A, Roy S. 2017. High altitude population of *Arabidopsis thaliana* is more plastic and adaptive under common garden than controlled condition. *BMC Ecology* **17**: 39.

Stuart Y, Veen T, Weber J, Hanson D, Ravinet M, Lohman BK, Thompson CL, Tasneem T, Doggett A, Izen R *et al.* 2017. Contrasting effects of environment and genetics generate a continuum of parallel evolution. *Nature Ecology & Evolution* **1**: 0158.

Suter L, Rüegg M, Zemp N, Hennig L, Widmer A. 2014. Gene regulatory variation mediates flowering responses to vernalization along an altitudinal gradient in *Arabidopsis*. *Plant Physiology* **166**: 1928–1942.

Suzuki N, Mittler R. 2006. Reactive oxygen species and temperature stresses: a delicate balance between signaling and destruction. *Physiologia Plantarum* **126**: 45–51.

Tabas-Madrid D, Méndez-Vigo B, Arteaga N, Marcer A, Pascual-Montano A, Weigel D, Pico XF, Alonso-Blanco C. 2018. Genome-wide signatures of flowering adaptation to climate temperature: regional analyses in a highly diverse native range of *Arabidopsis thaliana*. *Plant, Cell & Environment* **41**: 1806–1820.

Takahashi Y, Zhang J, Hsu PK, Ceciliato PHO, Zhang L, Dubeaux G, Munemasa S, Ge C, Zhao Y, Hauser F *et al.* 2020. MAP3Kinase-dependent SnRK2-kinase activation is required for abscisic acid signal transduction and rapid osmotic stress response. *Nature Communications* **11**: 12.

Therneau T. 2012. *The lmekin function*. Rochester, MN, USA: Mayo Clinic.

Tian F, Yang D-C, Meng Y-Q, Jin J, Gao G. 2019. PlantRegMap: charting functional regulatory maps in plants. *Nucleic Acids Research* **48**: D1104–D1113.

Tripathi AM, Singh A, Singh R, Verma AK, Roy S. 2019. Modulation of miRNA expression in natural populations of *A. thaliana* along a wide altitudinal gradient of Indian Himalayas. *Science Reports* **9**: 441.

Tusiime FM, Gizaw A, Gussarova G, Nemomissa S, Popp M, Masao CA, Wondimu T, Abdi AA, Mirré V, Muwanika V *et al.* 2020. Afroalpine flagships revisited: parallel adaptation, intermountain admixture, and shallow genetic structuring in the giant senecios (*Dendrosenecio*). *PLoS ONE* **15**: e0228979.

Tyagi A, Yadav A, Tripathi AM, Roy S. 2016. High light intensity plays a major role in emergence of population level variation in *Arabidopsis thaliana* along an altitudinal gradient. *Science Reports* **6**: 26160.

Vidigal DS, Marques ACSS, Willems LAJ, Buijs G, Méndez-Vigo B, Hilhorst HWM, Bentsink L, Picó FX, Alonso-Blanco C. 2016. Altitudinal and climatic associations of seed dormancy and flowering traits evidence adaptation of annual life cycle timing in *Arabidopsis thaliana*: climatic adaptation of annual life cycles. *Plant, Cell & Environment* **39**: 1737–1748.

de Villemereuil P, Mouterde MM, Gaggiotti OE, Till-Bottraud I. 2018. Patterns of phenotypic plasticity and local adaptation in the wide elevation range of the alpine plant *Arabis alpina*. *Journal of Ecology* **106**: 1952–1971.

Wang H, Prentice IC, Davis TW, Keenan TF, Wright IJ, Peng C. 2017. Photosynthetic responses to altitude: an explanation based on optimality principles. *New Phytologist* **213**: 976–982.

Ward JK, Strain BR. 1997. Effects of low and elevated CO_2 partial pressure on growth and reproduction of Arabidopsis thaliana from different elevations. *Plant, Cell & Environment* **20**: 254–260.

Wei T, Simko V. 2021. *R package 'corrplot': Visualization of a correlation matrix*, v.0.92. [WWW document] URL https://github.com/taiyun/corrplot.

Wise RR. 1995. Chilling-enhanced photooxidation: the production, action and study of reactive oxygen species produced during chilling in the light. *Photosynthesis Research* **45**: 79–97.

Wolfe MD, Tonsor SJ. 2014. Adaptation to spring heat and drought in northeastern Spanish *Arabidopsis thaliana*. *New Phytologist* **201**: 323–334.

Wood SN. 2011. Fast stable restricted maximum likelihood and marginal likelihood estimation of semiparametric generalized linear models. *Journal of the Royal Statistical Society (B)* **73**: 3–36.

Wos G, Arc E, Hülber K, Konečná V, Knotek A, Požárová D, Bertel C, Kaplenig D, Mandáková T, Neuner G *et al.* 2022. Parallel local adaptation to an alpine environment in *Arabidopsis arenosa*. *Journal of Ecology* **110**: 2448–2461.

Yang J, Wang X, Gu H. 2024. Genetic basis of variation of flowering time in Tibetan *Arabidopsis thaliana*. *Chinese Bulletin of Botany* **59**: 373–382.

Yim C, Bellis ES, DeLeo VL, Gamba D, Muscarella R, Lasky JR. 2023. Climate biogeography of *Arabidopsis thaliana*: linking distribution models and individual variation. *Journal of Biogeography* **00**: 1–15.

Zheng X, Levine D, Shen J, Gogarten SM, Laurie C, Weir B. 2012. A high-performance computing toolset for relatedness and principal component analysis of SNP data. *Bioinformatics* **28**: 3326–3328.

Zhou X, Stephens M. 2012. Genome-wide efficient mixed-model analysis for association studies. *Nature Genetics* **44**: 821–824.

Zhu Y, Siegwolf RT, Durka W, Körner C. 2010. Phylogenetically balanced evidence for structural and carbon isotope responses in plants along elevational gradients. *Oecologia* **162**: 853–863.

Supporting Information

Additional Supporting Information may be found online in the Supporting Information section at the end of the article.

Dataset S1 Ecotypes coordinates, elevation, and region.

Dataset S2 Environmental variables used in the PCA of Fig. (1b).

Dataset S3–S5 Experiments Percival programs and HOBO data.

Dataset S6 Datasets of phenotypes used in this study.

Dataset S7 Top SNPs and annotations in Flowering Time GWAS.

Dataset S8 Top SNPs and annotations for the low pCO_2 GWAS.

Dataset S9 Top SNPs and annotations for the high-light GWAS.

Dataset S10 Top SNPs and annotations for the night-freezing GWAS.

Methods S1 Sequencing, variant calling, and genomic datasets.

Methods S2 Initial growing conditions.

Methods S3 Experiment 1 conditions and phenotypes.

Methods S4 Experiments 2 and 3 conditions and phenotypes.

Notes S1 Regional classification and regional differences.

Notes S2 Analysis of RGB color data.

Notes S3 Regional trait variation and covariation.

Notes S4 GWAS for antioxidant activity.

Fig. S1 Flowering time and genes regional variation.

Fig. S2 PCA of color phenotypes.

Fig. S3 Trait–elevation clines within Asia and W Mediterranean.

Fig. S4 Manhattan and QQplots (PDF).

Fig. S5 GWAS results for antioxidant activity under high light.

Fig. S6 Regional DOG1 haplotype variation.

Fig. S7 GAMs of trait–elevation clines across the native range.

Table S1 Subsampled LM for trait–elevation clines.

Table S2 GO enrichment of genes assigned to 100 top GWAS SNPs.

Table S3 Western Mediterranean QTL climate enrichment.

Table S4 Asia QTL climate enrichment.

Please note: Wiley is not responsible for the content or functionality of any Supporting Information supplied by the authors. Any queries (other than missing material) should be directed to the *New Phytologist* Central Office.